Drug Development and Industrial Pharmacy, 22(9&10), 909-916 (1996)

Properties of Solid Dispersions of Naproxen in Various Polyethylene Glycols

P. Mura,* A. Manderioli, G. Bramanti, and L. Ceccarelli

Dipartimento di Scienze Farmaceutiche, Universita' di Firenze, Via G. Capponi 9, 50121 Firenze, Italy

ABSTRACT

Solid dispersions of naproxen in polyethylene glycol 4000, 6000, and 20000, aimed at improving the drug dissolution characteristics, were prepared by both the solvent and melting methods. The drug–polymer interaction in the solid state was investigated using differential scanning calorimetry, hot-stage microscopy, Fourier-transform infrared spectroscopy, and x-ray diffraction analysis. Interaction in solution was studied by phase solubility analysis and dissolution experiments. Computer-aided molecular modeling was used to supplement the results from phase solubility studies. No important chemical interaction was found between naproxen and polyethylene glycol, either in solution or in the solid state, apart from the formation of weak drug–polymer hydrogen bonds. The increase of naproxen dissolution rate from its binary systems with polyethylene glycol could be attributed to several factors such as improved wettability, local solubilization, and drug particle size reduction. No influence of polymer molecular weight or of the solid dispersion preparation method on drug dissolution properties was found.

INTRODUCTION

The solid dispersion approach has been widely and successfully applied to improve the solubility, dissolution rates, and consequently the bioavailability of poorly water-soluble drugs. Of the numerous substances examined for their carrier properties, one of the most commonly used is polyethylene glycol.

Polyethylene glycols (PEGs) are mixtures of condensation polymers of ethylene oxide and water. The repeating unit is oxyethylene ($O–CH_2–CH_2–$), with either end of the chain comprising a hydroxyl group. Various

*To whom correspondence should be addressed.

molecular weight fractions have been scrutinized as solid dispersion carriers, from PEG 400 to PEG 35000. However, comparison of the relative effectiveness of PEGs of different molecular weight does not allow a general conclusion, because conflicting results have been reported (1–5). It may thus be concluded that the influence of PEG molecular weight on drug dissolution characteristics is as yet unpredictable.

Continuing our studies aimed at improving the dissolution characteristics of naproxen (a nonsteroid antiinflammatory drug with very low water solubility), where both PVP (6) and cyclodextrins (7,8) were used as carriers, we thought that it would be of interest to investigate the properties of binary systems of naproxen and PEG of different average molecular weights (4000, 6000, 20000). This involved the study of the possible interaction between naproxen and PEG both in solution and in the solid state. Interaction in the solid state was investigated by differential scanning calorimetry (DSC), hot-stage microscopy, x-ray diffraction analysis, and Fourier-transform infrared (FT-IR) spectroscopy. Interaction in solution was studied by phase solubility analysis and dissolution experiments, and complemented by computer-aided molecular modelling.

MATERIALS AND METHODS

Materials

Naproxen (NAP) (Sigma Chemical Co., St. Louis, MO, USA) and polyethylene glycol (PEG) 4000, 6000, and 20000 (Merck, Darmstadt, Germany) were used as obtained from the suppliers. All other materials and solvents were of analytical reagent grade.

Preparation of NAP–PEG Binary Systems

1. Physical mixtures: Physical mixtures of NAP and PEG powders were prepared in different ratios by simple mixing in an agate mortar with a spatula proper amounts of the two components previously sieved (75–150 μm).

2. Cofused systems: Confused systems were prepared by heating, with constant stirring, NAP–PEG physical mixtures until they all melted. The melts were quickly cooled and solidified on an ice bath. The dispersions were stored 48 h in a desiccator under vacuum at room temperature before being ground in an agate mortar with a pestle and sieved (75–150 μm).

3. Coevaporated systems: Coevaporated systems were prepared by dissolving NAP–PEG physical mixtures in a minimum volume of methanol. The solvent was then removed by evaporation in vacuum at 37°C. The dispersions were kept 24 h in a desiccator under vacuum at room temperature and then ground and sieved (75–150 μm).

Investigation Techniques

Thermal Analysis

Temperature and enthalpy measurements were performed with a Mettler TA4000 apparatus equipped with a DSC 25 cell at a scanning rate of 10 K min^{-1}, on 5-10-mg (Mettler M3 microbalance) samples in pierced Al pans under static air.

Hot-Stage Microscopy

Approximately 1–3 mg of sample was placed on a microscope slide and heated at 5–10 K min^{-1} on a Koffler Hot-Stage fitted on Reichert Thermover microscope. The completion of melting was considered as the final disappearance of solid.

X-ray Diffraction

X-ray powder diffraction patterns were obtained with a Philips PW 1130 diffractometer (CuK_α radiation), at a scan rate of 2° min^{-1} over the 5–40 2θ range.

Infrared Analysis

Fourier-Transform infrared (FT-IR) spectra (KBr disk) were obtained on a Perkin-Elmer Model 1710 apparatus using Fourier transformations of 10 scans. The instrument was internally calibrated with a laser.

Solubility Studies

Solubility measurements of NAP were carried out by adding an excess of drug (15 mg) to 15 mL of water or aqueous solution of PEG (from 2% to 10% w/v), in sealed glass containers which were electromagnetically stirred at constant temperature until equilibrium was achieved (2 days). An aliquot was withdrawn and filtered (pore size 0.45 μm), and the NAP concentration was determined by a second derivative ultraviolet absorption method at 274 nm (6). The presence of PEG did not exhibit any interference. Three temperatures were tested (25°, 37°, and 45°C) and each experiment was performed in triplicate.

Molecular Modeling

Analysis and modeling of NAP and PEG molecules was carried out using the INSIGHT 2.2.0 program (Byosim Technologies) (9). The structure was subjected to a process of energy minimization (Consistent Valence Force Field, DISCOVER 2.9.5 program), performing iterations to a <0.01 derivative value. Docking energy was calculated at -273°C.

Dissolution Studies

Dissolution rates of NAP, alone or from the various binary systems with each PEG, were determined in water at 37 ± 0.3°C according to the dispersed amount method. NAP or NAP equivalent, 20 mg, was added to 300 mL of bidistilled water, in a 400-mL beaker. Stirring was provided by a three-blade (19 mm diameter) glass stirrer rotating at 100 rpm, immersed in the beaker at 2.5 cm from the bottom. At suitable time intervals, 3.0 mL samples were withdrawn, filtered (pore size 0.45 μm), and spectrophotometrically assayed for NAP content as in the solubility studies. The same volume of fresh medium was added and the correction for the cumulative dilution was calculated. Each test was repeated four times (coefficient of variation, CV < 1.5%).

RESULTS AND DISCUSSION

Interaction in the Solid State

The DSC curves of the pure products (Fig. 1) exhibited a single endothermic effect, corresponding to the melting of NAP (T_{fus} 156.2°C, $\Delta_f H$ 135 J g^{-1}) or polymer (T_{fus} 59.6°C, $\Delta_f H$ 175 J g^{-1} for PEG 4000; T_{fus} 61.0°C, $\Delta_f H$ 197 J g^{-1} for PEG 6000; T_{fus} 62.6°C, $\Delta_f H$ 168 J g^{-1} for PEG 20000). Each sample, cooled to room temperature, crystallized out, and exhibited substantially the same thermal behavior in a second heating run.

For each NAP–PEG binary system (see, e.g., the series of physical mixtures in Fig. 2), DSC curves of combinations containing an excess weight fraction of NAP showed two endothermal transitions. The former was always peaked very close to the PEG melting temperature (monotectic melt); the latter corresponded to the drug melting. When the drug content was decreased, the endothermic peak corresponding to the drug melting gradually shifted to a lower temperature and broadened, losing its sharp, distinct appearance. As the drug–polymer ratio further decreased, the DSC curves showed

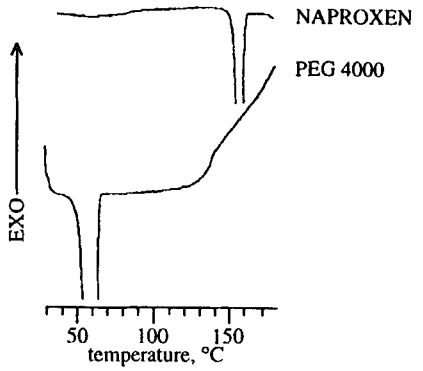

Figure 1. DSC curves of the pure products (naproxen and PEG 4000).

the only one endothermic peak, corresponding to the melting of the polymer. NAP–PEG systems were found to be completely miscible in the liquid phase and completely immiscible in the solid state, as was also confirmed by hot-stage microscopy.

Solid dispersions (either cofused or coevaporated systems) showed the same thermal behavior as the physical mixtures of the same composition. The similarities between the DSC data for the solid dispersions and the corresponding physical mixtures, as shown in Fig. 3 for all the 50:50 w/w NAP–PEG binary systems, indicated the absence of a well-defined chemical interaction between NAP and PEG.

Typical equilibrium phase diagrams, constructed using peak melting points and hot-stage microscopy data, are shown in Fig. 4. They revealed no evidence of the

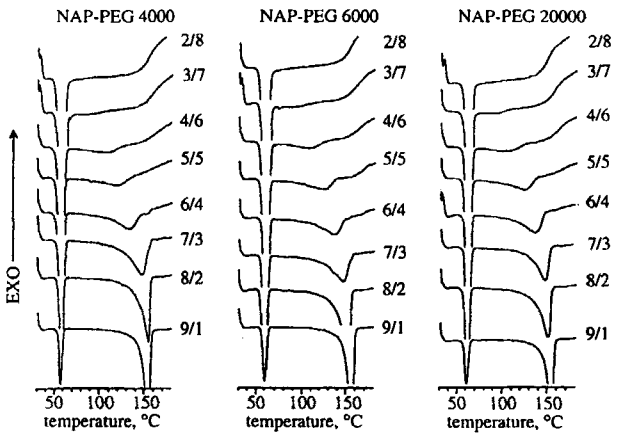

Figure 2. DSC curves of naproxen (NAP)–PEG physical mixtures of different drug-to-polymer (w/w) ratios.

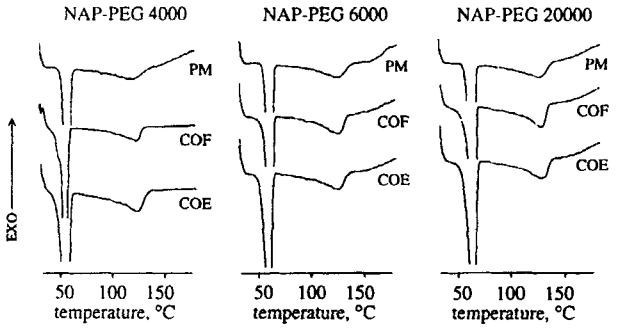

Figure 3. DSC curves of naproxen (NAP)–PEG 50:50 w/w physical mixture (PM), and coevaporated (COE) and cofused (COF) systems.

presence of eutectics or solid solutions and were all of the monotectic type, the monotectic species being the pure drug. This indicates that the melts are miscible, but that there is a negligible interaction in the solid state. The rising liquid curve corresponded to the drug solubility in the liquid PEG. All other phase diagrams showed similar profiles and were almost independent of the PEG molecular weight and of the method used to prepare a given drug–polymer mixture.

X-ray diffraction analysis showed that crystalline PEG and crystalline NAP were detectable in all the drug–polymer solid binary systems, confirming their immiscibility in the solid state. No presence of amorphous phases was observed either in coevaporated or in cofused systems. Major x-ray diffraction peaks of NAP were, in fact, present in the various physical mixtures as well as in the cofused and coevaporated systems, even if some of these were covered by the peaks of the polymer. Moreover the 2θ angles of the PEG reflections were practically unchanged. The diffraction peaks of NAP were again recognizable also in NAP–PEG 10:90 w/w systems, as shown, for example, in Fig. 5 for NAP–PEG 4000 binary systems. The similar heights of the NAP diffraction peaks in the physical mixtures and in the corresponding solid dispersions confirmed the negligible solid solubility of NAP in the polymer, as also found by thermal studies. The absence in cofused and coevaporated products of any x-ray diffraction peaks, other than those attributed to pure NAP and PEG, also indicated a lack of a well-defined chemical interaction between drug and carrier in their solid state.

Representative FT-IR spectra of pure components, NAP and PEG 4000, and their 50:50 w/w physical mixtures and cofused systems are shown in Fig. 6. The physical mixture spectrum was the weighted average of those of the single components. Only a weak modification in the characteristic quartet of NAP frequency bands in the carbonyl stretching region (1730–1600 cm^{-1}) was observed by comparing the spectra of physical mixtures with those of corresponding solid dispersion systems. This might well be indicative of a weak involvement of this group in hydrogen bonding interaction in the solid dispersions. A similar behavior was observed also for PEG 6000 and 20000.

Interaction in Aqueous Phase

In order to gain information on the nature of a possible interaction in solution between NAP and each carrier, solubility experiments were performed at three different temperatures (25°, 37°, and 45°C). The drug solubility linearly increased as the polymer concentration increased, in all cases showing the features of an A_L-type solubility phase diagram (Fig. 7). These results are consistent with the formation of soluble complexes (10) between NAP and PEG. No attempt was made to calculate the apparent stability constants, since the exact stoichiometrical relationship of drug/polymer con-

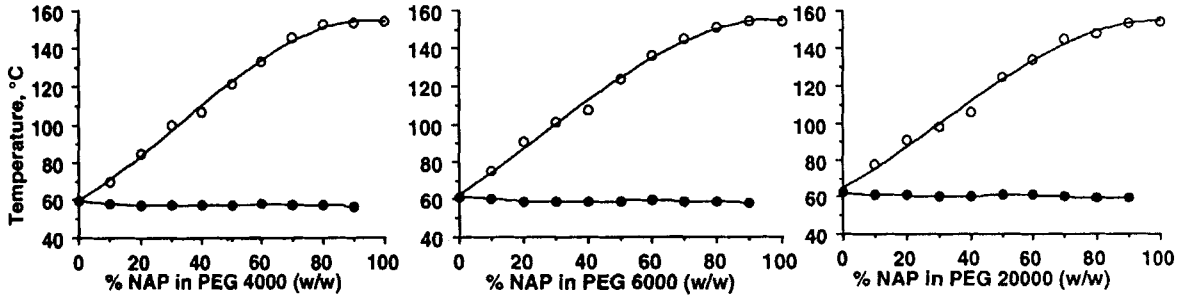

Figure 4. Phase diagrams of physical mixtures of naproxen (NAP) and PEG 4000, 6000, and 20000, constructed using DSC analysis and hot-stage microscopy.

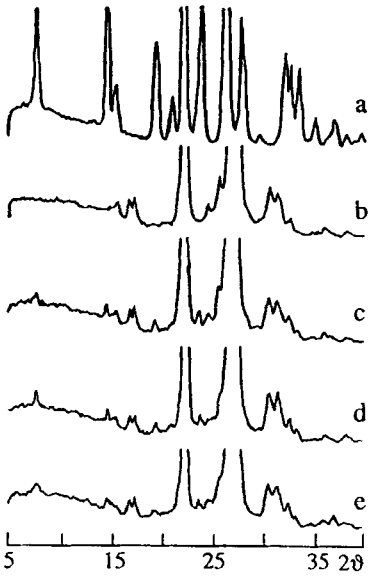

Figure 5. X-ray powder diffraction patterns of naproxen (NAP) (a); PEG 4000 (b); and their 10:90 w/w physical mixtures (c); and cofused (d) and coevaporated (e) systems.

centration ratio should be known. Based on data from solubility diagrams, the ratio for the number of molecules of the polymer required to solubilize 1 molecule of NAP was 68, 60, and 25 for PEG 4000, 6000, and

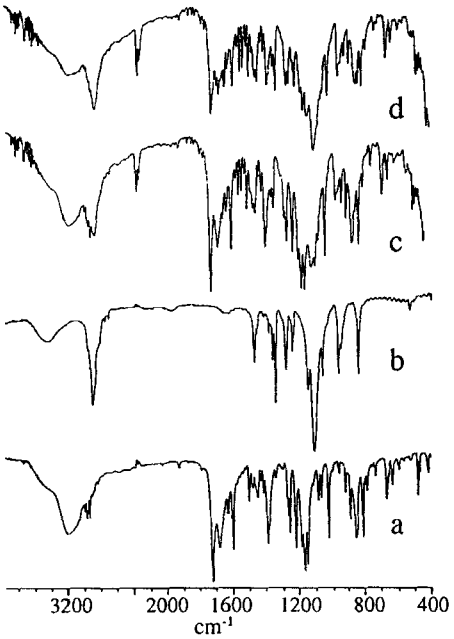

Figure 6. FT-IR spectra of naproxen (NAP) (a); PEG 4000 (b); and their 50:50 w/w physical mixtures (c); and cofused systems (d).

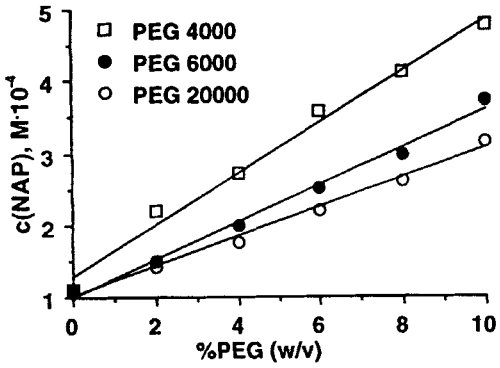

Figure 7. Aqueous solubilities of naproxen (NAP) in the presence of PEG at 25°C. Key: (□) PEG 4000; (●) PEG 6000; (○) PEG 20000.

20000, respectively, indicating the formation of very weak complexes with high dissociation constants (11). However, a qualitative comparison of the degrees of interaction of the various PEGs was possible. The slopes of the straight-line relationships are in fact, indicative of the relative affinity of the drug for the polymer (12). These were decreased by increasing both the polymer molecular weight and the temperature. PEG 4000 always showed the best solubilizing power, with about a fourfold increase in drug solubility.

Thermodynamic parameters for the process of NAP dissolution in PEG aqueous solutions (Table 1) were determined from the variation of drug solubility at each PEG concentration as a function of the temperature. The values of log N/N_0 (where N and N_0 represent the mole fraction solubility of NAP in aqueous solution, with and without PEG present) were plotted against the inverse of the absolute temperature. The enthalpy values were calculated from the slopes of these plots (13); the free energy variation and the change in entropy associated with the dissolution process were evaluated using classic thermodynamic equations.

The drug dissolution process was found to be exothermic and thermodynamically favored by the negative enthalpy variation. The ΔH values found (ranged between -10 and -25 kJ/mol) suggested a weak involvement of hydrogen bonds in the NAP-polymer interaction in solution (14).

Computer-generated structures of PEG and NAP, with their van der Waals surfaces, are given in Fig. 8. In the case of the PEG structure, the dihedral angles values of C-O bonds (about 180°) and C-C bonds (about 60°) were fixed in accordance with data reported in the literature (15-17), thus obtaining the regular sym-

Table 1

Thermodynamic Parameters for the Dissolution of Naproxen (NAP) in PEG Aqueous Solutions

	ΔG (J/mol)			ΔH	ΔS
	25°C	37°C	45°C	(kJ/mol)	(J/mol K)
% PEG 4000					
2	-1705	-1146	-673	-16.9	-51.1
4	-2251	-1600	-1142	-18.6	-55.1
6	-2936	-2032	-1495	-24.5	-72.4
8	-3289	-2320	-1850	-24.9	-72.6
10	-3637	-2654	-2155	-25.9	-74.7
% PEG 6000					
2	-751	-664	-137	-9.3	-28.8
4	-1469	-1054	-473	-15.8	-48.1
6	-2050	-1499	-710	-21.5	-65.1
8	-2478	-2020	-992	-23.6	-70.8
10	-3039	-2474	-1493	-25.3	-74.7
% PEG 20000					
2	-650	-540	-104	-8.3	-25.7
4	-1165	-927	-311	-13.2	-40.5
6	-1718	-1093	-504	-19.5	-59.8
8	-2160	-1562	-684	-23.5	-71.8
10	-2615	-1905	-1040	-25.5	-76.8

metrical helical structure which represents an energy minimum situation and is the most generally accepted molecular geometry (18). After the minimization process of NAP and PEG interacting molecules, as a consequence of the reciprocal interaction, the NAP molecule, oriented itself as shown in Fig. 9, causing a distortion of the PEG helical structure. Docking energy value for the interaction between NAP and PEG was -5.5 kJ/mol, due to the contribution of both van der Waals and electrostatic forces (-3.3 kJ/mol and -2.2 kJ/mol, respectively).

The results of dissolution rate tests, performed according to the dispersed amount method on 10:90 w/w drug-polymer physical mixtures and solid dispersions

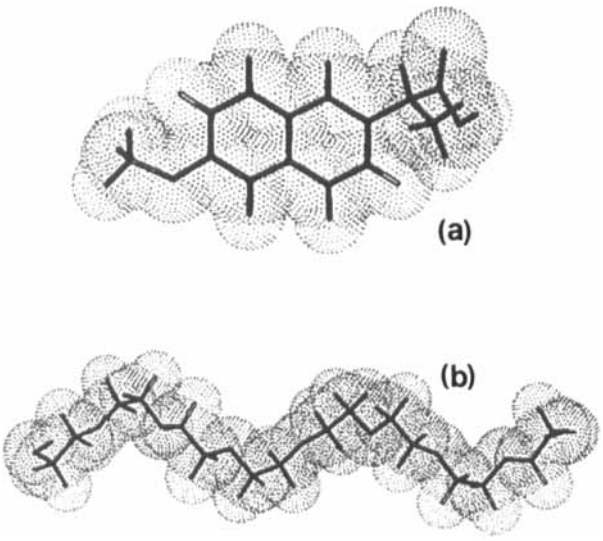

Figure 8. Computer-generated structure of naproxen (a) and PEG (b) molecules.

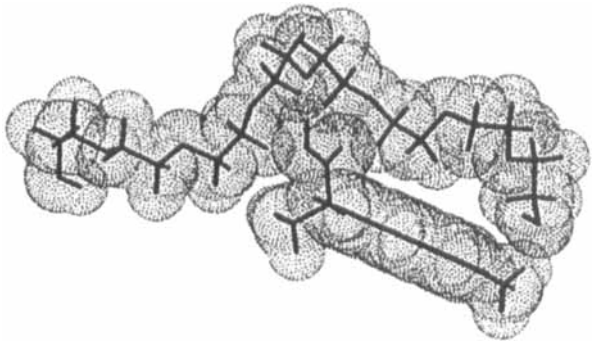

Figure 9. Computer-generated structure representing the naproxen (NAP)-PEG interaction.

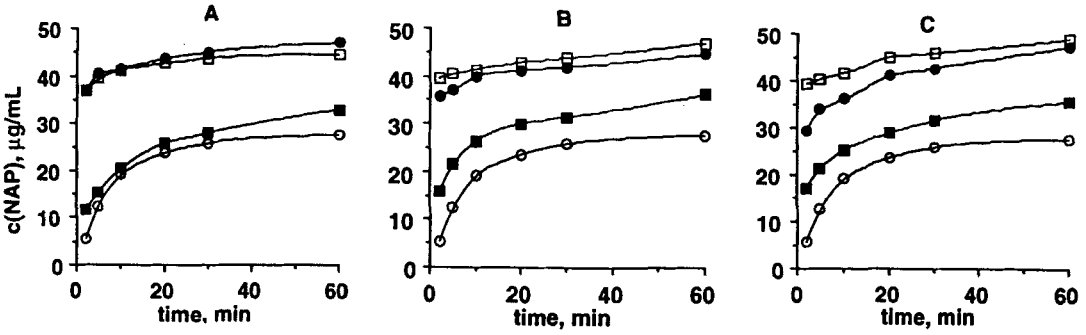

Figure 10. Dissolution profiles of naproxen (NAP) from 10:90 w/w drug–polymer ratio binary systems with PEG 4000 (A), PEG 6000 (B) and PEG 2000 (C) in water at 37°C. Key: (○) NAP alone; (■) physical mixtures; (●) cofused systems; (□) coevaporated systems.

(cofused and coevaporated systems), are shown in Fig. 10. NAP dissolution was always faster from solid dispersions than from physical mixtures, and both were faster than pure drug dissolution. No significant differences in NAP dissolution rate were observed between cofused and coevaporated systems, and the drug release rate was almost independent of the PEG molecular weight. It may be observed that the increase in dissolution rate is greater at first as the PEG present dissolves and is then depressed by the large amount of drug already in the dissolution medium. The increase in the dissolution of the drug when it is physically mixed with PEG is probably due to a wettability improvement and a local solubilization effect by the carrier at the diffusion layer. The further increased dissolution in the case of the dispersed drug could be attributed to other factors, such as absence of aggregation or agglomeration phenomena and particle size reduction.

Because the influence of these factors may depend on the polymer content in the dispersed systems, the effect of NAP–PEG 4000 composition on the drug release rate from cofused systems was determined and NAP relative dissolution rate (calculated at 10 min, referring to that of pure NAP) was plotted as a function of the drug content (Fig. 11). At a very high polymer concentration, a prevailing viscosity delaying effect was observed (19), and the percent of drug dissolved after a given time linearly increased by increasing its content in solid dispersions up to 10% w/w (20–23). A broad optimum was then reached, ranging between 10% and 20% of drug content, probably indicating a saturation of the process involved in drug removal from the dissolving dispersion (20). Above this concentration, slower dissolution rates were observed.

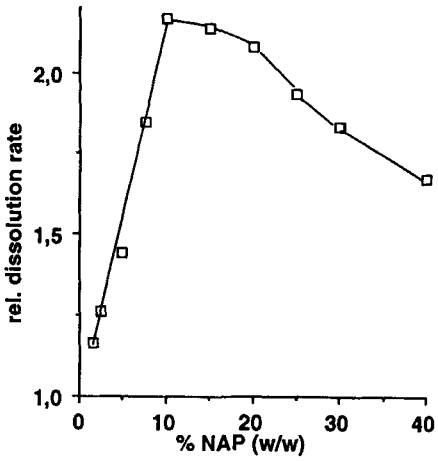

Figure 11. Relative dissolution rate (at 10 min) of naproxen (NAP) from cofused systems with PEG 4000 as a function of drug content.

CONCLUSIONS

The results of solid-state studies revealed the absence of any chemical decomposition and of a well-defined chemical interaction between the drug and the carrier as a consequence of fusion or coevaporation processes, indicating compatibility between PEGs and NAP as well as the possibility of using them as carriers for NAP solid dispersions.

Phase solubility studies showed a solubilizing effect by the carrier. The negative free energy variation which accompanied the NAP dissolution process in PEG aqueous solutions was found to be due to a favorable negative enthalpy variation, which suggested the involvement of a weak hydrogen bond between drug and carrier.

PEGs were found to be less effective in improving NAP dissolution properties than the previously tested carriers: i.e., PVP (6) and cyclodextrins (7,8). This could partly be explained by the fact that, unlike the systems obtained with PVP and cyclodextrins, dispersed systems prepared using PEGs did not appear to contain any amorphous drug. On the other hand, the presence of crystalline drug should ensure the higher stability of NAP–polymer binary systems in time.

ACKNOWLEDGMENT

Financial support from the MURST (60%) is gratefully acknowledged.

REFERENCES

1. J. L. Ford, A. F. Stewart, and J. L. Dubois, Int. J. Pharm., 28, 11 (1986).
2. D. Q. M. Craig and J. M. Newton, Int. J. Pharm., 78, 175 (1992).
3. M. Sumnu, STP Pharma, 2, 299 (1986).
4. P. Mura, A. Liguori, and G. Bramanti, Farmaco Ed. Pr., 42, 149 (1987).
5. A. S. Geneidi, M. S. Adel, and E. Shehate, Can. J. Pharm. Sci., 15, 78 (1980).
6. G. P. Bettinetti, P. Mura, A. Liguori, and G. Bramanti, Farmaco Ed. Pr., 11, 331 (1988).
7. G. P. Bettinetti, P. Mura, A. Liguori, and G. Bramanti, Il Farmaco, 2, 197 (1989).
8. G. P. Bettinetti, A. Gazzaniga, P. Mura, F. Giordano, and M. Setti, Drug Dev. Ind. Pharm., 18, 39 (1992).
9. Biosym Technologies, 9685 Scranton Road, San Diego, CA 92121-2777.
10. T. Higuchi, and K. A. Connors, Adv. Anal. Chem. Instr., 4, 117 (1965).
11. W. L. Chiou, J. Pharm. Sci., 66, 989 (1977).
12. N. M. Najib and M. S. Suleiman, Int. J. Pharm., 51, 225 (1989).
13. M. Shahjahan and R. P. Enever, Int. J. Pharm., 82, 229 (1992).
14. S. Feldman and M. Gibaldi, J. Pharm. Sci., 56, 370 (1967).
15. S. I. Mizushima and T. Shimanouchi, J. Polym. Sci., 86, 3521 (1964).
16. J. Maxfield and I. W. Shepherd, Polymer, 16, 505 (1975).
17. E. Delaite, J. J. Point, P. Damman, and M. Dosière, Macromolecules, 25, 4768 (1992).
18. G. Heun and J. Breitkrentz, Pharmazie, 49, 562 (1994).
19. I. W. Kellaway and N. N. Najib, Int. J. Pharm. Tech. Prod. Mfr., 4, 37 (1983).
20. J. L. Ford, A. F. Stewart, and J. L. Dubois, Int. J. Pharm., 28, 11 (1986).
21. J. L. Ford, Pharm. Acta Elv., 59, 280 (1984).
22. J. Fernandez, J. L. Vila-Jato, J. Blanco, and J. L. Ford, Drug. Dev. Ind. Pharm., 15, 2491 (1989).
23. J. L. Dubois and J. L. Ford, J. Pharm. Pharmacol., 37, 494 (1985).